Breast Cancer: Targets and Therapy

Dovepress
Taylor & Francis Group

Open Access Full Text Article

ORIGINAL RESEARCH

CLEC3A Promotes Immune Evasion and Tumor Progression by Enhancing PD-L1 Stability to Weaken T Cell Cytotoxicity in Luminal Breast Cancer

Chen Chen[1–3], Hongtao Li[2], Yuan Liu[2], Xiaojing Zhang[2], Yanfeng Sun[2], Xianming Li[1,3]

[1]Jinan University, Guangzhou, Guangdong, 510632, People's Republic of China; [2]Department of Surgical Oncology, The First Affiliated Hospital of Bengbu Medical University, Bengbu, Anhui, 233000, People's Republic of China; [3]Department of Radiation Oncology, The 2nd Clinical Medical College (Shenzhen People's Hospital) of Jinan University, Shenzhen, Guangdong, 518020, People's Republic of China

Correspondence: Xianming Li, Department of Radiation Oncology, The 2nd Clinical Medical College (Shenzhen People's Hospital) of Jinan University, No. 1017 Dongmenbei Road, Luohu District, Shenzhen, Guangdong, 518020, People's Republic of China, Email lxm1828@hotmail.com

Breast Cancer: Targets and Therapy downloaded from https://www.dovepress.com/
For personal use only.

Background: Luminal breast cancer (BC) is the most common subtype of BC. C-type lectin domain family 3 member A (CLEC3A) has been shown to promote malignant characteristics in BC cells, but the specific mechanisms are not well understood. This study aimed to explore the oncogenic role of CLEC3A in luminal BC and its potential mechanisms.

Methods: Transcriptomic data from GEO and TCGA databases were analyzed to identify differentially expressed genes in luminal BC. Kaplan–Meier curves were used to assess the prognostic value of CLEC3A in luminal BC, and CLEC3A expression was further validated in BC cell lines. Functional assays, including colony formation, wound healing, Transwell, and flow cytometry, were performed following CLEC3A knockdown or overexpression. The impact of CLEC3A on PD-L1 stability was analyzed by co-immunoprecipitation (co-IP) and Western blotting. The influence of CLEC3A on T cell activity was investigated by co-culturing $CD8^+$ T cells with BC cells.

Results: CLEC3A expression was significantly upregulated in luminal BC patients and correlated with poor overall survival. In vitro, CLEC3A knockdown suppressed proliferation, migration, invasion and promoted apoptosis, whereas CLEC3A overexpression enhanced these malignant features. CLEC3A also regulated mRNA expression levels of key proliferation-related genes and immune factors, and it regulated the stability of PD-L1 protein in BC cells through ubiquitination. Additionally, CLEC3A knockdown increased tumor cell death and CD8+ T cell activity, while overexpression suppressed these responses.

Conclusion: CLEC3A promotes BC progression and immune evasion by regulating PD-L1 stability and inhibiting CD8+ T cell function. Targeting CLEC3A may enhance anti-tumor immunity and improve patient outcomes in luminal BC.

Keywords: luminal breast cancer, CLEC3A, cancer progression, PD-L1, ubiquitination, tumor immune microenvironment

Introduction

Breast cancer (BC) is the most prevalent cancer among women globally. According to the 2020 Global Cancer Statistics, BC accounts for 11.7% of newly diagnosed cancer cases and 6.9% of cancer-related deaths.[1] BC exhibits high heterogeneity and can be classified into multiple subtypes based on receptor status, with the most common subtypes being luminal A and luminal B, characterized by estrogen receptor (ER) positivity, accounting for 65–70% of all invasive BC cases.[2–4] Despite significant advances in endocrine and targeted therapies, luminal BC remains clinically challenging: more than 40% of patients eventually relapse or lose their luminal/epithelial characteristics, leading to poorly differentiated tumors with enhanced invasiveness and metastatic potential.[1,5,6] Furthermore, the disease course in luminal BC is often prolonged, and late recurrence contributes to the fact that the 20-year survival rate is not markedly superior to that of other subtypes.[7] Given its high prevalence, distinctive pattern of late recurrence, and tendency toward

Received: 9 April 2025
Accepted: 13 October 2025
Published: 27 October 2025

© 2025 Chen et al. This work is published and licensed by Dove Medical Press Limited. The full terms of this license are available at https://www.dovepress.com/terms.php and incorporate the Creative Commons Attribution – Non Commercial (unported, v4.0) License (http://creativecommons.org/licenses/by-nc/4.0/). By accessing the work you hereby accept the Terms. Non-commercial uses of the work are permitted without any further permission from Dove Medical Press Limited, provided the work is properly attributed. For permission for commercial use of this work, please see paragraphs 4.2 and 5 of our Terms (https://www.dovepress.com/terms.php).

therapeutic resistance, it is critical to investigate the molecular mechanisms driving luminal BC progression to develop more precise and durable treatment strategies.

Increasing evidence has shown that the tumor microenvironment (TME) plays a crucial role in the progression of BC, with immune regulation in the TME being particularly important. Programmed death ligand-1 (PD-L1), as a major inhibitory checkpoint molecule, plays a critical role in this process. The PD-L1 expressed on tumor cells binds to the PD-1 receptor on immune cells, inhibiting T-cell-mediated anti-tumor responses, thereby helping tumor cells escape immune surveillance.[8] Although luminal BC is typically considered to have a moderate or low immune profile compared to other subtypes,[9] Deici et al reported that 9% of luminal A and 42% of luminal B cases exhibited PD-L1 immune reactivity.[10] Ni et al further pointed out that the expression of PD-L1 in tumor-infiltrating immune cells is associated with better prognosis in luminal B BC.[11] These findings suggest that immune regulation in luminal BC is more dynamic than previously thought. Post-translational modifications, especially ubiquitination, significantly affect the stability and function of PD-L1, thereby regulating its immune inhibitory effect.[12] Zhu et al found that deubiquitinating enzymes promote immune evasion in the BC cell line MCF-7 cells by preventing the degradation of PD-L1.[13] However, the precise molecular mechanisms by which ubiquitination regulates PD-L1 in luminal BC remain unclear.

C-type lectin domain family 3 member A (CLEC3A) is a cell surface protein involved in various immune processes. Previous studies have demonstrated that high expression of CLEC3A in invasive ductal carcinoma of the breast is associated with poor prognosis and promotes tumor progression.[14] More recently, CLEC3A has been identified as a driver of aggressiveness in both ER+ and ER− breast cancers.[15] In addition, Ni et al reported that CLEC3A overexpression enhances the proliferation, migration, and invasion of BT474 breast cancer cells.[16] Another study demonstrated that CLEC3A is an immune-related hub gene in BC.[17] However, despite these findings, the specific mechanisms by which CLEC3A promotes luminal BC progression, particularly its role within the TME, remain largely unknown. Based on prior evidence, we hypothesized that CLEC3A may regulate PD-L1 stability through ubiquitination, thereby contributing to immune evasion in luminal BC.

Therefore, the present study aimed to explore the molecular interactions between CLEC3A and PD-L1 and elucidate the potential role of CLEC3A as a therapeutic target for enhancing anti-tumor immunity in luminal BC.

Methods

Differentially Expressed Genes (DEGs) Screening

Expression profiles from the GEO dataset GSE115144 (total 42 samples, including 21 luminal BC tumor samples and 21 adjacent normal samples) and the TCGA-BC datasets (total 1180 samples, including 614 luminal BC and 88 normal breast tissue samples) were used in this study. DEGs were identified by using the limma R package. First, DEGs between luminal BC and normal samples were screened in the GSE115144 dataset with a threshold of $p<0.05$ and $|\log2 \text{ fold change (FC)}|>1.2$. Subsequently, the upregulated genes were further validated for differential expression between luminal BC and normal samples in the TCGA cohort, applying a threshold of $p<0.05$ and $|\log2 FC|>0.2$. The results were visualized in the volcano plot and heatmap using the ggplot2 package.

Clustering Analysis

Consensus clustering based on Non-negative Matrix Factorization (NMF) was performed using the expression profiles of DEGs to classify luminal BC samples into different molecular subgroups. The optimal number of clusters was determined according to the cophenetic correlation coefficient, dispersion, and silhouette width. Subsequently, NMF feature weight matrices were used to identify key contributors within each cluster. Kaplan-Meier (KM) survival analysis was conducted using survminer and survival R packages to compare the overall survival (OS) between different clusters. A heatmap for hub gene expression in different clusters was generated using the pheatmap R package, and violin plots comparing the expression of hub genes across clusters were generated using ggplot2.

Evaluation of Prognostic Implications and Immune Correlation

The expression levels of hub genes in normal and tumor tissues were evaluated using the TCGA-BC dataset. Statistical analysis was performed using the Wilcoxon rank-sum test. Survival analysis for hub genes was conducted based on high and low expression levels. Hazard ratios (HR) were calculated using the Cox proportional hazards model, and KM survival curves were plotted. The correlation between hub genes and the immune checkpoint gene CD274 (PD-L1) was analyzed using Spearman correlation and visualized using scatter plots.

Immunohistochemistry (IHC) Assay

IHC was performed to evaluate CLEC3A expression in paraffin-embedded tissues. Sections (4 μm) were deparaffinized, rehydrated, and subjected to antigen retrieval in Tris-EDTA buffer. Endogenous peroxidase activity was blocked with 0.3% hydrogen peroxide for 10 min, followed by incubation with 5% normal goat serum for 30 min. Slides were then incubated overnight at 4°C with a rabbit anti-CLEC3A antibody, washed, and treated with HRP-conjugated secondary antibody for 30 min at room temperature. Signal detection was performed using 3,3′-diaminobenzidine and counter-stained with hematoxylin. The expression of CLEC3A was evaluated according to the percentage of positive cells.

Cell Culture and Treatment

Human normal mammary epithelial cells MCF 10A and Human luminal BC cell lines MCF-7 (luminal A) and BT-474 (luminal B) were purchased from the Wuhan Pricella Biotechnology Co., Ltd. (Wuhan, China). All cells were cultured in DMEM (Sigma-Aldrich, MO, USA) supplemented with 10% fetal bovine serum (FBS) and 1% penicillin/streptomycin at 37°C in a 5% CO_2 incubator.

Cell Transfection

For CLEC3A stable knockdown in MCF-7 and BT-474 cells, lentiviral vectors carrying short hairpin RNA targeting CLEC3A (sh-CLEC3A) and the negative control (shNC) were obtained from GenePharma (Shanghai, China), and transfected cells were selected using puromycin (Clontech, USA). To achieve CLEC3A overexpression in MCF-7 and BT-474 cells, the pcDNA3.1-CLEC3A plasmid was transfected into the cells by Lipofectamine 2000. Expression levels were verified by real-time quantitative PCR (RT-qPCR) analysis after 48 h of transfection.

Cell Viability Analysis

Cell viability was assessed using the cell counting kit-8 (CCK-8) assay (Beyotime, Shanghai, China). MCF-7 and BT-474 cells were seeded at a density of 5×10^3 cells per well in 96-well plates. Following the treatment for 12 h, 24 h, 48 h, or 72 h, 10 μL of CCK-8 solution was added to each well and the cells were incubated for an additional 2 h at 37°C. The absorbance at 450 nm was measured using a microplate reader (BioTek, USA).

Tunnel Assay for Cell Apoptosis

The TUNEL assay was performed to detect apoptotic cells in MCF-7 and BT-474 cells. Cells were fixed with 4% paraformaldehyde for 30 min at room temperature and washed with PBS. Cells were then permeabilized with 0.1% Triton X-100 in PBS for 5 min. Subsequently, the TUNEL reaction mixture, containing terminal deoxynucleotidyl transferase (TdT) and biotinylated dUTP, was added to the cells and incubated for 60 min at 37°C in a humidified chamber. Afterward, the cells were washed with PBS and incubated with streptavidin-HRP (Horseradish peroxidase) for 30 min at room temperature. The apoptotic cells were visualized by adding the DAB substrate, which turns the apoptotic cells brown due to the enzymatic reaction. The number of TUNEL-positive cells was counted under a light microscope, and the apoptosis rate was calculated as the percentage of TUNEL-positive cells relative to the total number of cells.

Colony Formation Assay

Transfected cells were seeded at a density of 2.5×10^5 cells per well in 24-well plates. Every three days, the medium was refreshed. Colony formation was monitored under an optical microscope (AE2000, Motic, China). After two weeks, cells

were fixed with 4% paraformaldehyde at 4°C for 1 h and then washed with PBS. Crystal violet staining solution was added to the wells to stain the colonies. Following a thorough wash with PBS, colony images were captured using a camera (Canon Ltd., Japan). The number of colonies was counted microscopically.

Wound Healing Assay

MCF-7 and BT-474 cells were seeded into 6-well plates at a density of 1×10^6 cells per well. A sterile 200 μL pipette tip was used to create a straight scratch in the center of the cell monolayer. After wounding, the medium was replaced with serum-free DMEM to prevent further cell proliferation. The cells were then incubated at 37°C with 5% CO_2. Images of the wound area were taken at 0 and 24 h under a microscope to observe cell migration into the wound area. The wound closure was quantified by measuring the distance between the wound's edges using image analysis software.

Transwell Assay for Cell Invasion

Cells were starved overnight in a serum-free medium and then resuspended in the same medium. The upper chamber of the Transwell insert (Corning, NY, USA) was coated with Matrigel (BD Biosciences, NJ, USA). A total of 1×10^4 cells in 200 μL serum-free medium were added to the upper chamber, while the lower chamber contained 600 μL of DMEM with 10% FBS. The cells were incubated for 24 h at 37°C with 5% CO_2. After incubation, non-invading cells were removed from the upper surface of the membrane. The invading cells on the lower surface of the membrane were fixed with 4% paraformaldehyde for 30 min, stained with crystal violet for 30 min, and then washed with PBS. The invaded cells were counted under a microscope. The invasive ability was quantified by calculating the average number of invaded cells.

Cycloheximide (CHX) Chase Assay

For the CHX chase assay, MCF-7 and BT-474 cells transfected with sh-CLEC3A were treated with 50 μg/mL CHX and harvested at 0, 4, 8, and 12 h post-treatment. The resulting lysates were analyzed by Western blotting using anti-CLEC3A and anti-GAPDH antibodies to assess protein degradation and stability.

RT-qPCR Assay

Total RNA was extracted using TRIzol reagent (Invitrogen, CA, USA) following the manufacturer's protocol. Reverse transcription was performed using the PrimeScript™ RT Reagent Kit (Takara, Japan) to synthesize complementary DNA (cDNA) from 1 μg of total RNA in a 20 μL reaction volume. The resulting cDNA was then used for qPCR, which was conducted using SYBR™ Green PCR Master Mix (Thermo Fisher, CA, USA) on a QuantStudio™ 7 Flex Real-Time PCR System (Applied Biosystems, CA, USA). The reaction was performed in a 20 μL volume containing 10 μL SYBR Green PCR Master Mix, 0.5 μL of each primer (10 μM), 2 μL of cDNA, and 7 μL of RNase-free water. The PCR conditions included an initial denaturation step at 95°C for 2 min, followed by 40 cycles of 95°C for 5 s and 60°C for 30s. The relative gene expression was calculated using the $2^{-\Delta\Delta Ct}$ method, with GAPDH as the internal control. The primer sequences are shown in Table S1.

Western Blotting Analysis

Cells were lysed using RIPA buffer (Thermo Fisher, CA, USA). The total protein concentration was determined using the BCA Protein Assay Kit (Thermo Fisher, CA, USA). Equal amounts of protein (20 μg) were separated by 10% SDS-PAGE and transferred to PVDF membranes (Beyotime, Shanghai, China). The membranes were blocked with 5% non-fat dry milk in TBST buffer for 1 h at room temperature. Membranes were then incubated overnight at 4°C with primary antibodies: anti-PD-L1 (Abcam, Cambridge, UK) and anti-GAPDH (Abcam, Cambridge, UK) as the loading control. After washing with TBST, the membranes were incubated with HRP-conjugated secondary antibodies for 1 h at room temperature. The protein bands were visualized using the ECL elements (Thermo Fisher, CA, USA) and captured with a chemiluminescence imaging system (Bio-Rad, CA, USA). The band intensities were quantified using ImageJ software, and the relative expression levels of PD-L1 were normalized to GAPDH.

Co-Culture for $CD8^+$ T Cells with BC Cell Lines

To evaluate the interaction between $CD8^+$ T cells and BC cell lines, a co-culture system was established using activated human $CD8^+$ T cells and MCF-7 or BT-474 cells. $CD8^+$ T cells were isolated from peripheral blood using a $CD8^+$ T Cell Isolation Kit (Miltenyi Biotec, Germany) and activated with anti-CD3 and anti-CD28 antibodies for 24 h in a complete medium. After activation, the $CD8^+$ T cells were co-cultured with the BC cell lines at a ratio of 1:1 in a Transwell system, allowing for indirect interaction between the T cells and tumor cells while preventing direct cell contact.

Crystal Violet Assay for Cell Viability

The Crystal Violet assay was used to assess the viability of BC cells after different treatments. Cells were seeded in 6-well plates at a density of 1×10^5 cells per well and allowed to grow for 24 h. After treatment, the cells were washed with PBS and fixed with 4% paraformaldehyde for 30–90 s at room temperature. The fixed cells were stained with 0.1% crystal violet solution (Sigma-Aldrich, USA) for 10–20 min at room temperature, followed by washing with PBS to remove excess dye. The number of alive tumor cells was quantified by counting the crystal violet-stained cells under a microscope. The stain was solubilized using 10% acetic acid for 1 h, and the absorbance was measured at 570 nm using a microplate reader.

Enzyme-Linked Immunosorbent Assay

The levels of IL-2 and TNF-γ in the supernatant of co-cultured cells were measured using ELISA kits (BioLegend, CA, USA), following the manufacturer's instructions. For the ELISA procedure, 96-well plates were coated overnight at 4°C with capture antibodies specific to IL-2 or TNF-γ. The plates were then blocked with 1% BSA in PBS for 1 h at room temperature. After washing, culture supernatant was added to the wells in duplicate, and standard curves were generated using recombinant IL-2 or TNF-γ. Plates were incubated for 2 h, followed by washing and the addition of a secondary HRP-conjugated detection antibody specific for IL-2 or TNF-γ, which was incubated for 1 h. After washing, the substrate solution (TMB) was added and incubated for 10 min in the dark. The reaction was stopped using the stop solution, and absorbance was measured at 450 nm using a microplate reader.

Flow Cytometry Assay

CD8+ T cells were collected after different treatments, washed with PBS, and stained with specific fluorochrome-conjugated antibodies to evaluate their functional status. T cell activation was assessed using anti-CD25-PE and anti-CD69-FITC antibodies. Proliferation was determined by CFSE labeling and analyzed by fluorescence dilution. Cytotoxic function was evaluated by intracellular staining with anti–Granzyme B-PC5.5 and anti–IFN-γ-PE antibodies. T cell exhaustion was assessed using anti–PD-1-FITC and anti–TIM3-PE antibodies. Samples were analyzed on a BD FACSCanto II flow cytometer, and data were processed with FlowJo software.

Statistical Analysis

Statistical analysis was performed using R (version 4.3.2) or GraphPad Prism (10.1.2). All experiments were performed at least in triplicates and data are presented as means ± standard deviation. Student's *t*-test was used for comparisons between two groups, and one-way ANOVA followed by Tukey's test was used for multiple comparisons. $p<0.05$ was considered statistically significant.

Results

Key Roles of CLEC3A and KLHDC7B in Molecular Subtyping of Luminal BC and Their Association with OS

Based on expression profiles from the GEO and TCGA databases, this study conducted DEG screening and clustering analysis for Luminal-type BC. First, 2958 DEGs were identified from the GSE115144 dataset, including 1665 upregulated and 1293 downregulated genes (Figure S1A and B). Then, the expression profiles of the 1665 upregulated genes

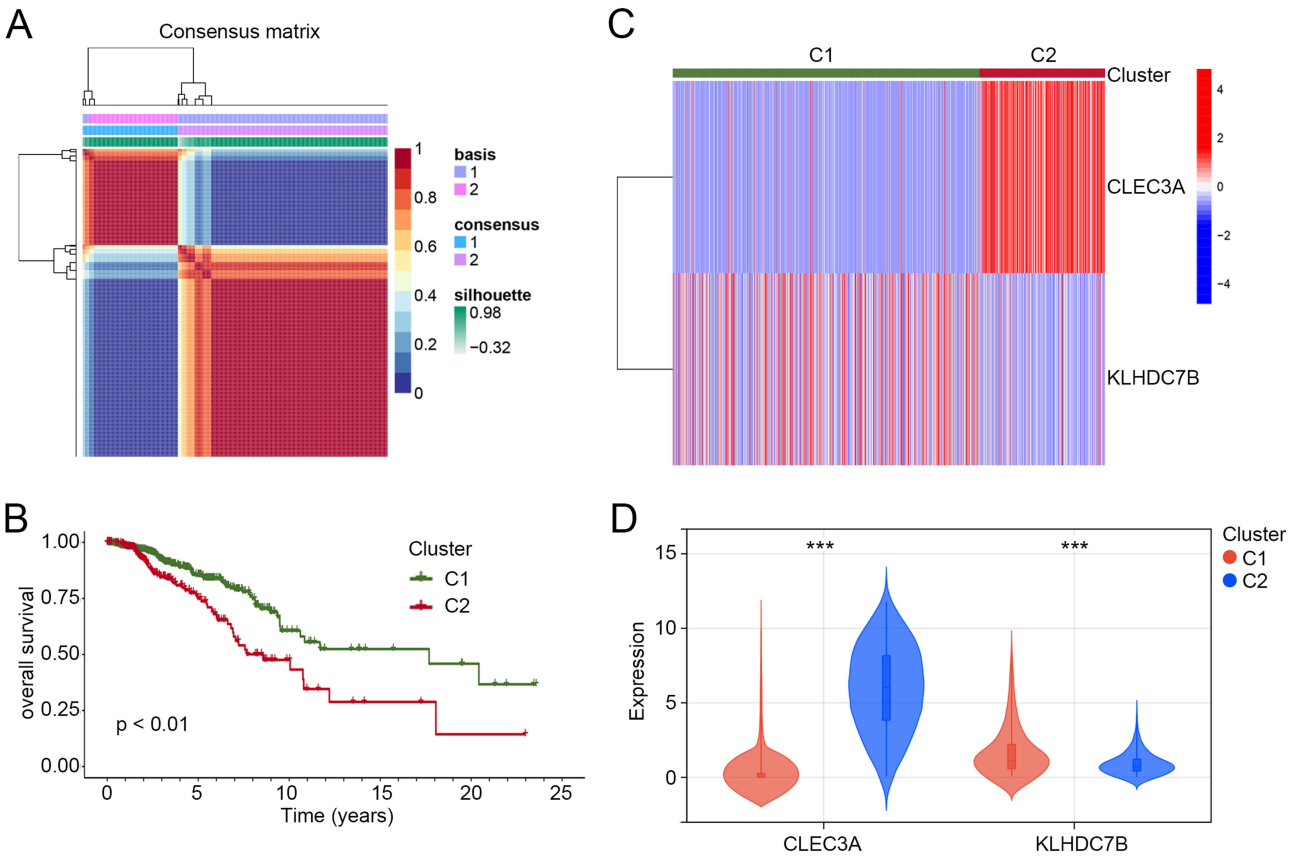

Figure 1 Key roles of CLEC3A and KLHDC7B in molecular subtyping of luminal BC and their association with overall survival. (**A**). Two molecular subtypes were identified. (**B**) Heatmap of CLEC3A and KLHDC7B's expression in two molecular subtypes. (**C**) Overall survival of breast cancer patients in two molecular subtypes. (**D**) Expression difference of CLEC3A and KLHDC7B in two molecular subtypes. ***p<0.001.

were extracted from TCGA-BC data, and differential analysis was performed again, resulting in 25 DEGs, including 12 upregulated and 13 downregulated genes (Figure S1C and D).

Based on the 25 DEGs expression data, consensus clustering analysis was applied to classify the samples. The analysis indicated that BC samples could be stably divided into two clusters (C1 and C2), and the consensus matrix showed high stability in clustering results (Figure 1A). Survival analysis indicated that patients in C2 had significantly lower OS than those in C1 ($p<0.01$, Figure 1B). Additionally, the clustering results revealed two representative genes, CLEC3A and KLHDC7B, with distinct expression patterns across the two clusters. CLEC3A expression was higher in C2 than in C1, whereas KLHDC7B exhibited the opposite expression pattern (Figure 1C). The violin plots further confirmed the opposite expression patterns of CLEC3A and KLHDC7B between the two clusters, with CLEC3A being significantly upregulated and KLHDC7B modestly downregulated in C2 ($p<0.001$, Figure 1D). These findings suggest that CLEC3A and KLHDC7B may play important roles in luminal BC subtyping. Therefore, CLEC3A and KLHDC7B were selected for further analyses.

Prognostic Implications and Immune Correlation of CLEC3A and KLHDC7B in Luminal BC

Next, the expression characteristics and prognostic significance of CLEC3A and KLHDC7B in BC were further explored. The results showed that both CLEC3A and KLHDC7B were significantly overexpressed in luminal BC compared to normal tissues ($p<0.05$, Figure 2A and B). Survival analysis indicated that patients with high CLEC3A expression had significantly worse OS compared to those with low expression ($p=0.011$, Figure 2C), and patients with high KLHDC7B expression exhibited better survival but without significance ($p=0.37$, Figure 2D). To further evaluate

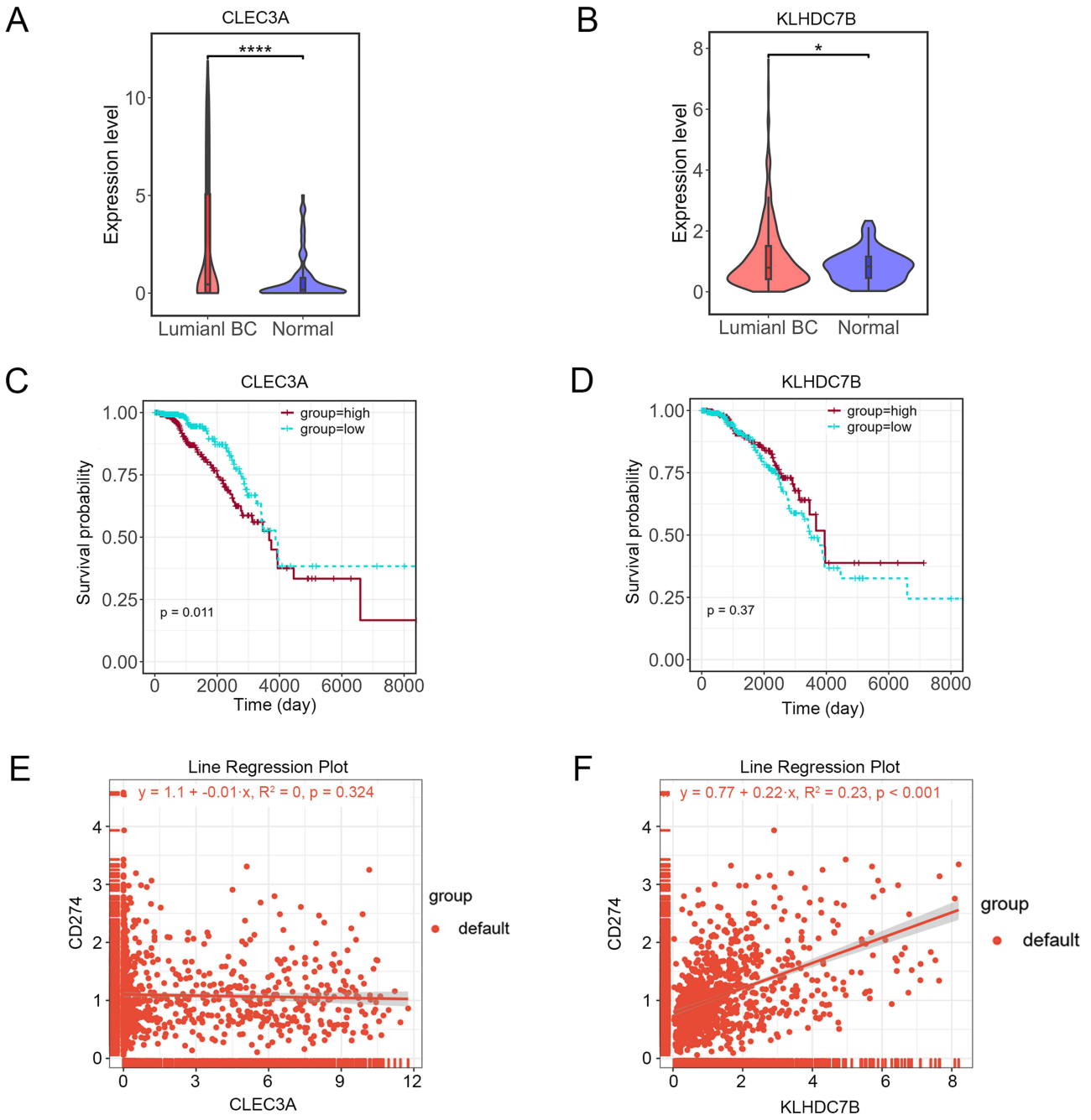

Figure 2 Prognostic implications and immune correlation of CLEC3A and KLHDC7B in BC. (**A** and **B**) Expression of CLEC3A and KLHDC7B in tumor and normal samples. (**C** and **D**) Overall survival of breast cancer patients in different expression levels of CLEC3A and KLHDC7B. (**E** and **F**) Correlation of CD274 with CLEC3A and KLHDC7B. ****p<0.0001.

the role of CLEC3A and KLHDC7B in immune regulation, their correlation with the immune checkpoint gene CD274 (PD-L1) was analyzed. The results showed that CLEC3A had no significant correlation with PD-L1 (R^2=0.01, p=0.324, Figure 2E), while KLHDC7B was positively correlated with CD274 (R^2=0.23, p<0.001, Figure 2F).

CLEC3A Was Upregulated in Luminal BC Cells and Promoted BC Cell Malignant Features

Subsequently, CLEC3A was selected for further validation because it was consistently upregulated in tumor tissues and the poor-prognosis cluster C2, and its high expression was significantly associated with worse OS. First, the expression

https://doi.org/10.2147/BCTT.S533474

differences of CLEC3A in normal and BC tissues and cells were examined. Compared with adjacent noncancerous tissues, the positive expression of CLEC3A was significantly increased in luminal BC tissues ($p < 0.001$, Figure S2A). Additionally, CLEC3A mRNA expression was significantly increased in the BC cell lines MCF-7 (luminal A) and BT-474 (luminal B) compared to the normal cell line MCF10A (Figure S2B). Therefore, sh-CLEC3A-1 and sh-CLEC3A-2 were transfected into MCF-7 and BT-474 cells to knock down CLEC3A expression. Figure 3A and B shows that compared to the shNC group, CLEC3A mRNA expression was significantly reduced in the sh-CLEC3A-1 and sh-CLEC3A-2 groups, indicating successful transfection. Additionally, cell viability was significantly lower ($p<0.05$, Figure 3C and D), and apoptosis rate was significantly higher ($p<0.01$, Figure 3E and F) in the sh-CLEC3A groups

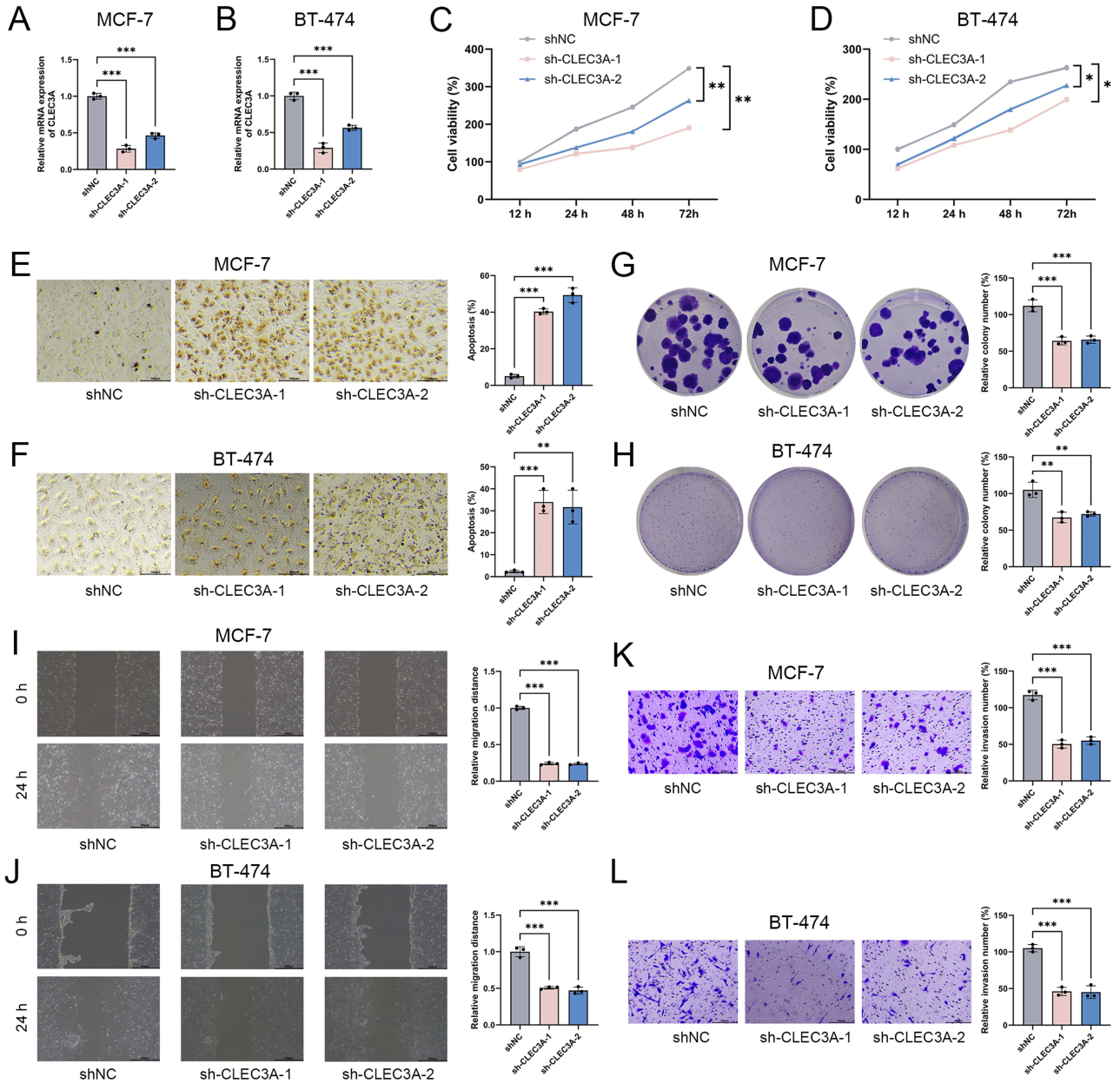

Figure 3 CLEC3A knockdown inhibited malignant behavior of BC cells. (**A** and **B**) mRNA expression of CLEC3A in MCF-7 and BT-474 cells.(**C** and **D**) Cell viability of MCF-7 and BT-474 cells. (**E** and **F**) Apoptosis of MCF-7 and BT-474 cells; scale bar = 100 μm. (**G** and **H**) Colony formation of MCF-7 and BT-474 cells. (**I** and **J**) Wound healing detected the migration of MCF-7 and BT-474 cells; scale bar = 500 μm. (**K** and **L**). Transwell detected the invasion of MCF-7 and BT-474 cells; scale bar = 200 μm. MCF-7 and BT-474 cells were transfected with sh-CLEC3A-1 or sh-CLEC3A-2. *p<0.05, **p<0.01, ***p<0.001.

 https://doi.org/10.2147/BCTT.S533474

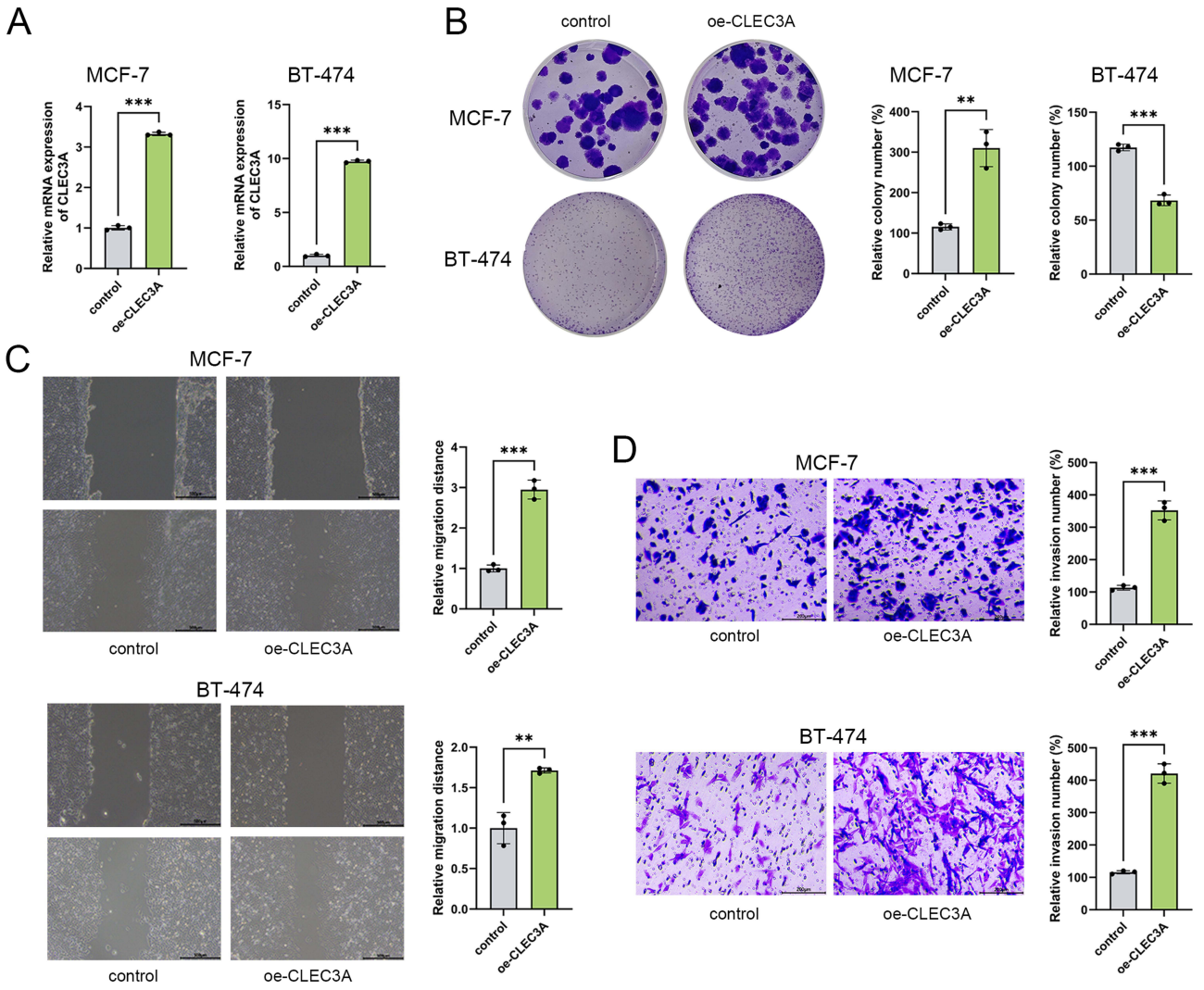

Figure 4 CLEC3A overexpression promoted malignant behavior of BC cells. (**A**) mRNA expression of CLEC3A in MCF-7 and BT-474 cells. (**B**) Colony formation of MCF-7 and BT-474 cells. (**C**) Wound healing detected the migration of MCF-7 and BT-474 cells; scale bar = 500 μm. (**D**) Transwell detected the invasion of MCF-7 and BT-474 cells; scale bar = 200 μm. MCF-7 and BT-474 cells were transfected with oe-CLEC3A. **p<0.01, ***p<0.001.

compared to the shNC group. CLEC3A knockdown also significantly decreased colony formation, migration, and invasion abilities of MCF-7 and BT-474 cells (p<0.001, Figure 3G–L).

To further validate the function of CLEC3A, CLEC3A was overexpressed in MCF-7 and BT-474 cells. After transfection with oe-CLEC3A, CLEC3A mRNA expression was successfully upregulated in MCF-7 and BT-474 cells (p<0.001, Figure 4A). Compared to the control group, the oe-CLEC3A group exhibited significantly enhanced cell proliferation, migration, and invasion (p<0.01, Figure 4B–D).

CLEC3A Regulated Expression of Cell Proliferation-Related Factors in Luminal BC Cells

Further investigation was conducted into how CLEC3A affects the expression of genes related to cell proliferation. CCND1, E2F1, MYC, and PCNA are associated with high proliferative capacity in cancer cells, while BCL2 is an anti-apoptotic factor and CDKN1A is a cell cycle inhibitor. The results showed that in MCF-7 cells, knockdown of CLEC3A (sh-CLEC3A-1 and sh-CLEC3A-2) significantly reduced the expression of CCND1, BCL2, E2F1, MYC, and PCNA, while markedly increasing the expression of CDKN1A, compared with the shNC control group (p<0.01, Figure 5A). Conversely, in the oe-CLEC3A group, compared to the control group, the expression of CCND1, BCL2, E2F1, MYC,

https://doi.org/10.2147/BCTT.S533474

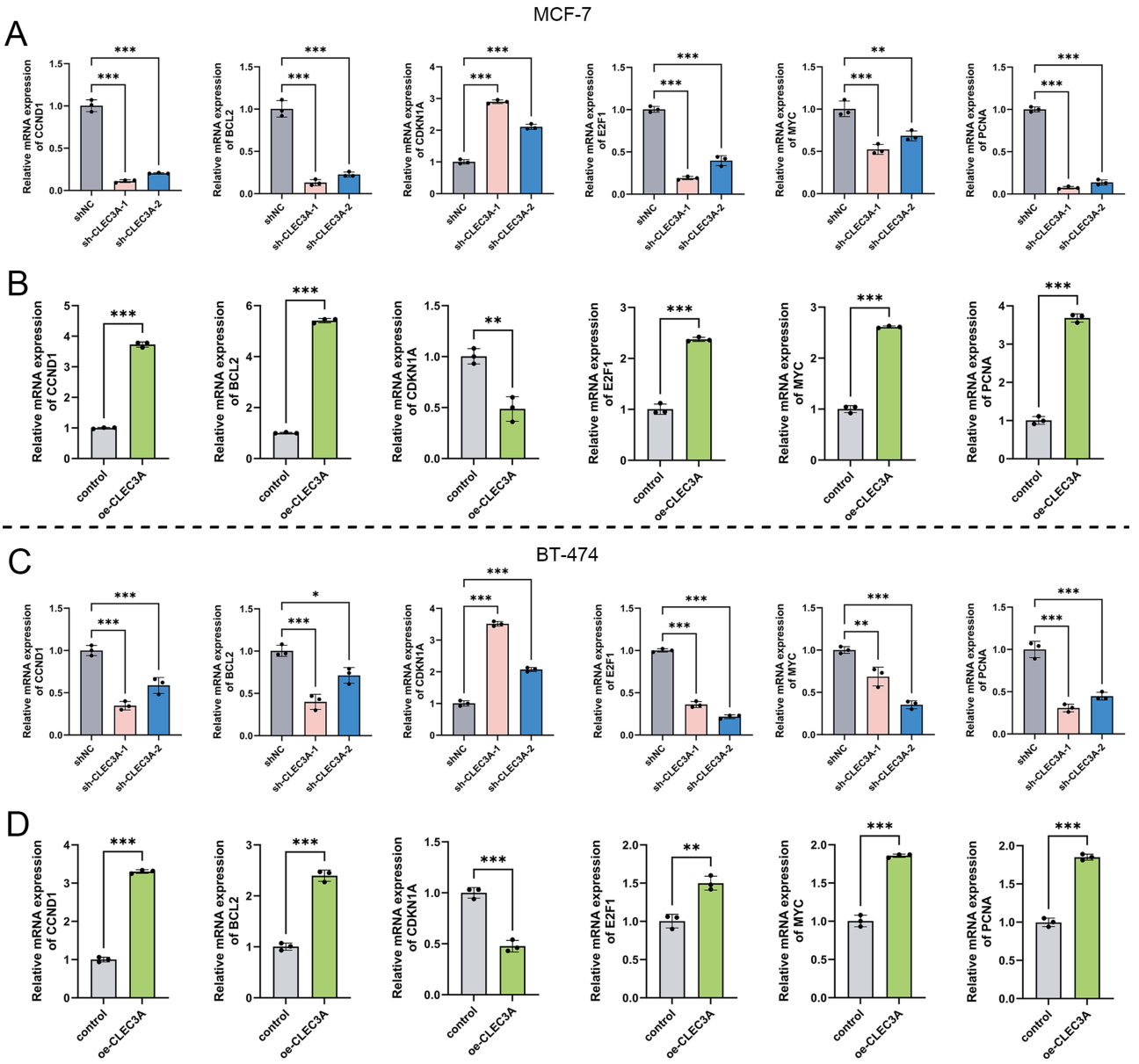

Figure 5 CLEC3A regulated expression of cell proliferation-related factors in BC cells. (**A**) mRNA expression levels of CCND1, BCL2, CDKN1A, E2F1, MYC, and PCNA in MCF-7 cells; MCF-7 cells were transfected with shNC, sh-CLEC3A-1, or sh-CLEC3A-2. (**B**) mRNA expression levels of CCND1, BCL2, CDKN1A, E2F1, MYC, and PCNA in MCF-7 cells; MCF-7 cells were transfected with oe-CLEC3A. (**C**) mRNA expression levels of CCND1, BCL2, CDKN1A, E2F1, MYC, and PCNA in BT-474 cells; BT-474cells were transfected with shNC, sh-CLEC3A-1, or sh-CLEC3A-2. (**D**) mRNA expression levels of CCND1, BCL2, CDKN1A, E2F1, MYC, and PCNA in BT-474 cells; BT-474 cells were transfected with oe-CLEC3A. *p<0.05, **p<0.01, ***p<0.001.

and PCNA was significantly upregulated, while CDKN1A expression was significantly downregulated (p<0.01, Figure 5B). Similar results were observed in BT-474 cells, where CLEC3A knockdown inhibited the expression of CCND1, BCL2, E2F1, MYC, and PCNA, and promoted CDKN1A expression (p<0.05, Figure 5C), while CLEC3A overexpression had the opposite effect (Figure 5D).

CLEC3A Regulated Expression of Immune-Related Factors in Luminal BC Cells

To explore the role of CLEC3A in the BC immune microenvironment, expression levels of key immune-related molecules (PD-L1, CXCL10, CCL2, IL2, IFNG, and STAT1) were examined. In both MCF-7 and BT-474 cells, CLEC3A knockdown significantly increased the mRNA expression of CXCL10, CCL2, IL2, IFNG, and STAT1, while CLEC3A overexpression suppressed their mRNA expression (Figure 6A–D). Notably, the changes in CLEC3A

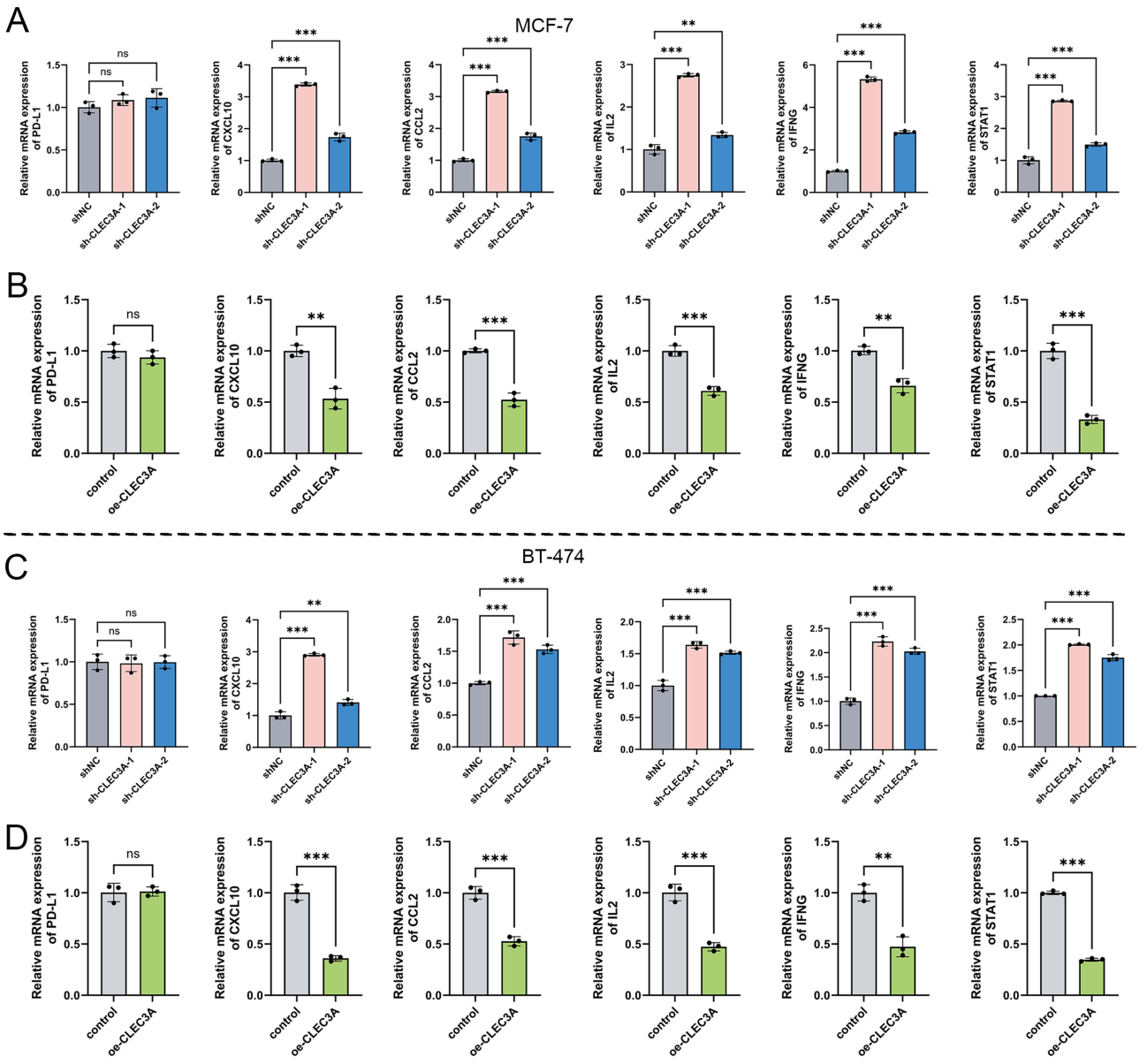

Figure 6 CLEC3A regulated expression of immune-related factors in BC cells. (**A**) mRNA expression levels of PD-L1, CXCL10, CCL2, IL2, IFNG, and STAT1 in MCF-7 cells; MCF-7 cells were transfected with shNC, sh-CLEC3A-1, or sh-CLEC3A-1.(**B**) mRNA expression levels of PD-L1, CXCL10, CCL2, IL2, IFNG, and STAT1 in MCF-7 cells; MCF-7 cells were transfected with oe-CLEC3A. (**C**) mRNA expression levels of PD-L1, CXCL10, CCL2, IL2, IFNG, and STAT1 in BT-474 cells; BT-474cells were transfected with shNC, sh-CLEC3A-1, or sh-CLEC3A-2. (**D**) mRNA expression levels of PD-L1, CXCL10, CCL2, IL2, IFNG, and STAT1 in BT-474 cells; BT-474 cells were transfected with oe-CLEC3A. **p<0.01, ***p<0.001, ns: no significance.

expression had no impact on PD-L1 mRNA expression, which was consistent with the above-mentioned correlation analysis results.

CLEC3A Regulated the Stability of PD-L1 Protein in Luminal BC Cells

To verify our hypothesis that CLEC3A may regulate PD-L1 through ubiquitination, we examined the protein levels of PD-L1. As shown in Figure 7A and B, CLEC3A knockdown significantly reduced PD-L1 protein expression, while CLEC3A overexpression increased PD-L1 protein levels ($p<0.01$). A protein synthesis inhibition experiment showed that CLEC3A knockdown accelerated the degradation rate of PD-L1 in CHX-treated MCF-7 cells, indicating that CLEC3A can affect PD-L1 stability (Figure 7B). Further analysis revealed that in the absence of a proteasome inhibitor (MG132), PD-L1 expression was significantly reduced in the CLEC3A knockdown group, but was significantly restored upon the

https://doi.org/10.2147/BCTT.S533474

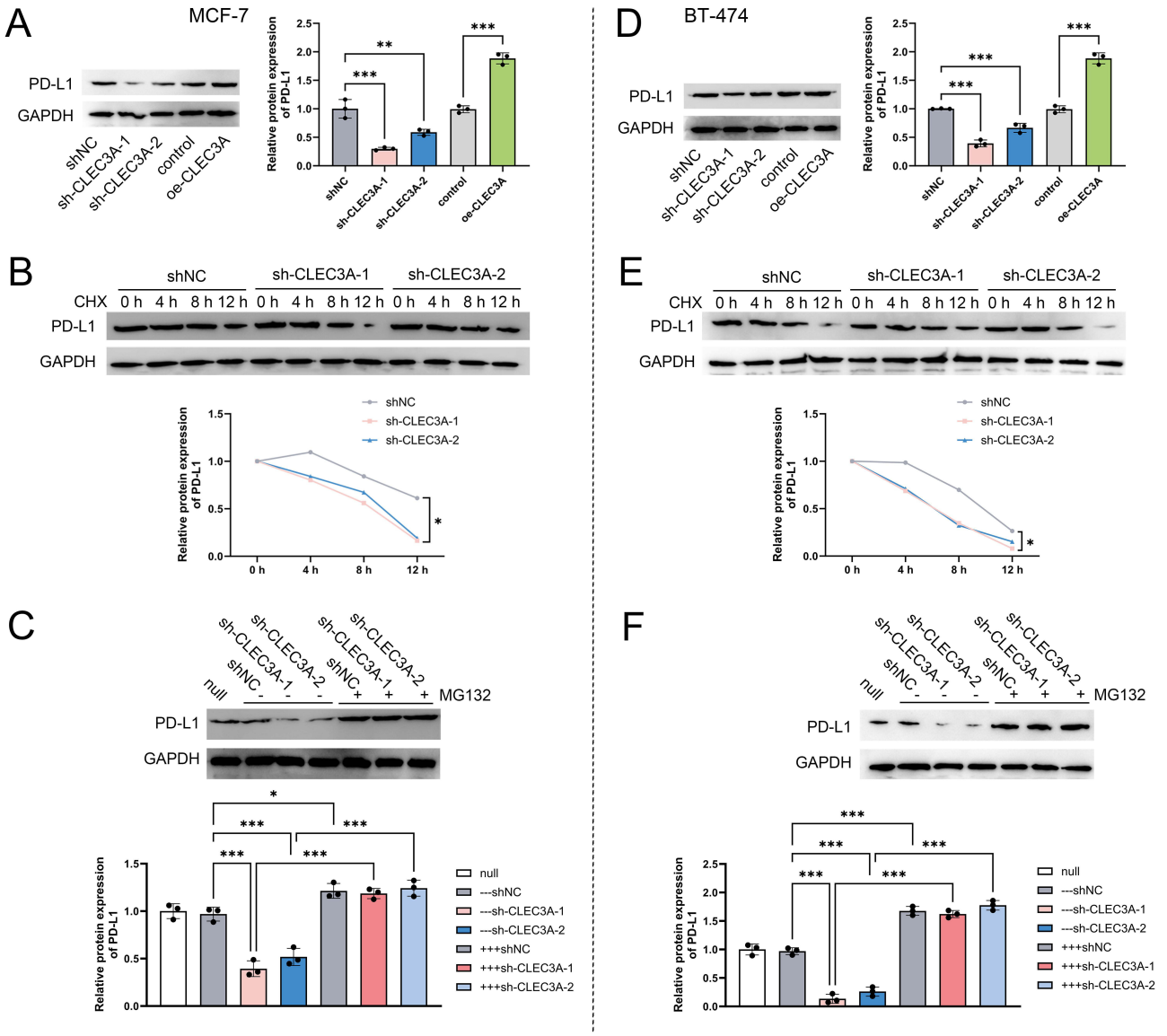

Figure 7 CLEC3A regulated the stability of PD-L1 protein in BC cells. (**A**–**C**) Protein expression of PD-L1 in MCF-7 cells; cells in (**A**) were transfected with sh-CLEC3A-1, sh-CLEC3A-2, or oe-CLEC3A; cells in (**B**) were transfected with sh-CLEC3A-1 or sh-CLEC3A-2 and treated with protein synthesis inhibitor CHX; cells in (**C**) were transfected with sh-CLEC3A-1 or sh-CLEC3A-2 and treated with/without proteasome inhibitor MG132. (**D**–**F**) Protein expression of PD-L1 in BT-474 cells; cells in (**D**) were transfected with sh-CLEC3A-1, sh-CLEC3A-2, or oe-CLEC3A; cells in (**E**) were transfected with sh-CLEC3A-1 or sh-CLEC3A-2 and treated with protein synthesis inhibitor CHX; cells in (**F**) were transfected with sh-CLEC3A-1 or sh-CLEC3A-2 and treated with/without proteasome inhibitor MG132. *p<0.05, **p<0.01, ***p<0.001.

addition of MG132, suggesting that CLEC3A regulates PD-L1 stability through a proteasome-mediated ubiquitination degradation pathway (Figure 7C). Similar results were observed in BT-474 cells (Figure 7D–F), further supporting CLEC3A's role in PD-L1 ubiquitination and degradation.

CLEC3A Affected the Luminal BC Immune Microenvironment by Regulating CD8+ T Cell Function

Next, we co-cultured activated human CD8+ T cells with MCF-7 or BT-474 cells to further assess the role of CLEC3A in the BC immune microenvironment. Functional assays revealed that inhibition of CLEC3A expression (sh-CLEC3A-1 and sh-CLEC3A-2) significantly enhanced the cytotoxic function of CD8+ T cells, evidenced by a significant increase in the proportions of CD8+-Perforin+ and CD8+-NF+ T cells (Figures 8A and B, 9A and B). Moreover, CLEC3A knockdown also significantly increased the tumor cell death rate in the co-culture system (Figures 8C and 9C), as well

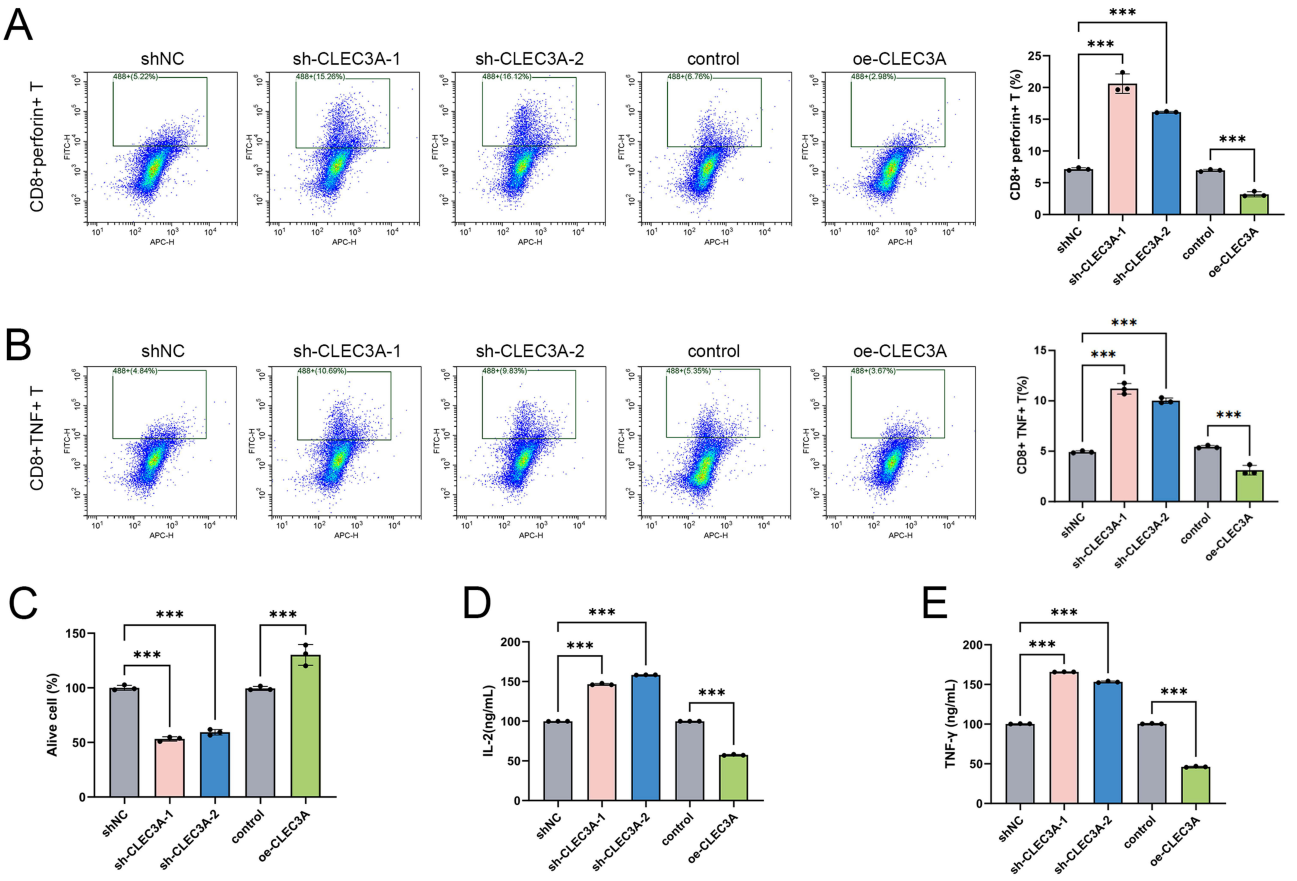

Figure 8 CLEC3A affected tumor immune microenvironment by regulating CD8+ T cell function in MCF-7 cells. (**A** and **B**) Detection of CD8+-Perforin+ and CD8+-NF+ T-cell levels by flow cytometry. (**C**) Alive cells of MCF-7. (**D** and **E**) Levels of IL-2 and TNF-γ. MCF-7 cells were transfected with sh-CLEC3A-1, sh-CLEC3A-2, or oe-CLEC3A. ***p<0.001.

as the secretion levels of IL-2 and TNF-γ (Figures 8D and E, 9D and E). In contrast, CLEC3A overexpression (oe-CLEC3A) significantly suppressed CD8+ T cell functions, including a reduced proportion of CD8+-Perforin+ and CD8+-TNF+ T cells, as well as decreased tumor cell death rate and cytokine secretion levels (Figures 8A–E and 9A–E). These results suggest that high CLEC3A expression may impair the anti-tumor function of CD8+ T cells by inhibiting their cytotoxicity and cytokine secretion, while CLEC3A knockdown significantly enhances the anti-tumor effects of CD8+ T cells.

CLEC3A Regulated CD8+ T Cell Function via PD-L1

To further elucidate the mechanism by which CLEC3A modulates CD8+ T cell function, we examined T cell activation, proliferation, cytotoxicity, and exhaustion in both MCF-7 and BT-474 cells. In MCF-7 cells, CLEC3A overexpression significantly reduced CD8+ T cell activation (CD69+, CD25+) (Figure 10A), proliferation (Figure 10B), and secretion of IFN-γ and Granzyme B (Figure 10C), while markedly increasing the proportion of exhausted PD-1+TIM3+ T cells (Figure 10D). Conversely, CLEC3A knockdown exerted the opposite effects, enhancing CD8+ T cell immune functions. Consistently, similar findings were observed in BT-474 cells: CLEC3A overexpression suppressed T cell activation, proliferation, and effector molecule secretion, whereas CLEC3A knockdown enhanced these functions (Figure 11A–D). Notably, blockade of PD-L1 or supplementation with recombinant PD-L1 could respectively reverse the functional changes induced by CLEC3A overexpression or knockdown, respectively (Figures 10A–D and 11A–D). These results suggest that CLEC3A may regulate the functional states of CD8 T cells through PD-L1, thereby promoting tumor immune evasion in luminal BC.

https://doi.org/10.2147/BCTT.S533474

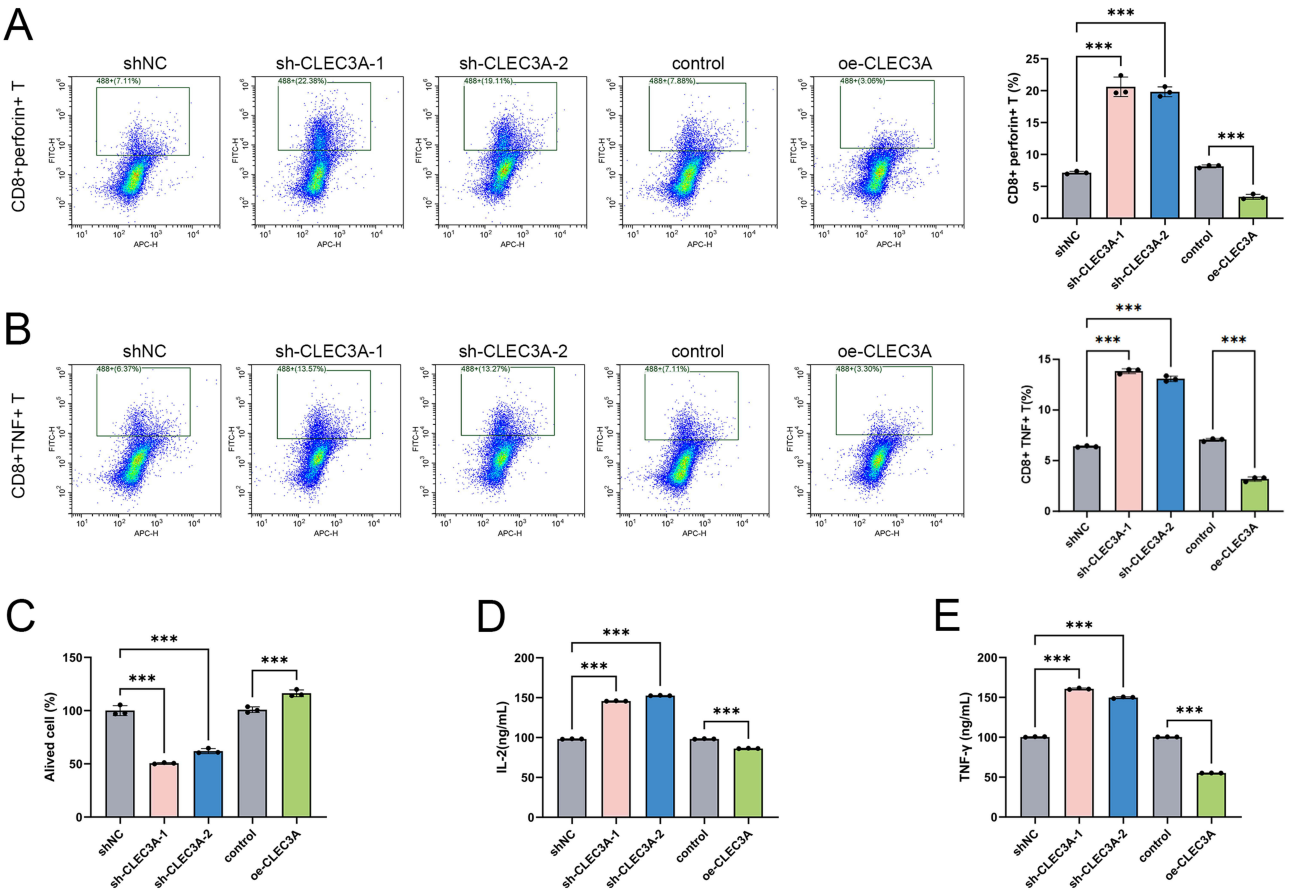

Figure 9 CLEC3A affected tumor immune microenvironment by regulating CD8+ T cell function in BT-474 cells. (**A** and **B**) Detection of CD8+-Perforin+ and CD8+-NF+ T-cell levels by flow cytometry. (**C**) Alive cells of BT-474. (**D** and **E**) Levels of IL-2 and TNF-γ. BT-474 cells were transfected with sh-CLEC3A-1, sh-CLEC3A-2, or oe-CLEC3A. ***p<0.001.

Discussion

In this study, we focused on the role of CLEC3A in luminal BC and its potential effects on prognosis, immune regulation, and tumor progression. Our results suggest that CLEC3A may be an important regulatory factor in BC, influencing cell proliferation, immune responses, and the stability of PD-L1, thereby shaping the tumor immune microenvironment.

By using bioinformatics analysis on the GEO and TCGA datasets, we clustered luminal BC patients into two subtypes, C1 and C2, with CLEC3A being a key gene in this classification. CLEC3A was first reported to be expressed in cartilage and later found to be a biomarker in various tumors, such as endometrial cancer,[18] pancreatic neuroendocrine tumors,[19] and lung cancer.[20] Several studies have reported the role of CLEC3A in the prognosis of BC. Chen et al identified CLEC3A as a risk gene in cuproptosis-related prognostic genes.[14] Another study indicated that low expression of CLEC3A was associated with improved OS in BC.[17] In our study, CLEC3A was upregulated in the C2 subtype, which had a worse prognosis. Survival analysis also showed that high CLEC3A expression was significantly associated with worsened OS in luminal BC patients, supporting its potential as a prognostic biomarker. To our knowledge, only Ni et al[16] have reported that CLEC3A promotes the proliferation, migration, and invasion of BC cells. In our study, CLEC3A expression was significantly upregulated in MCF-7 (luminal A) and BT-474 (luminal B) cells compared to normal cells. CLEC3A knockout significantly reduced cell viability, induced apoptosis, and decreased colony formation, migration, and invasion. Overexpression of CLEC3A enhanced the malignant behavior of MCF-7 and BT-474 cells. These results further confirm the findings of Ni et al,[16] supporting CLEC3A as a predictive biomarker for luminal BC progression. Zhang et al found that CLEC3A overexpression reduced G1 phase arrest in osteosarcoma cells.[21] Cell cycle dysregulation, characterized by the inactivation of tumor suppressors and abnormal activation of cyclins and cyclin-dependent kinases, is a hallmark of BC.[22] Our findings show that CLEC3A knockout leads to significant downregulation

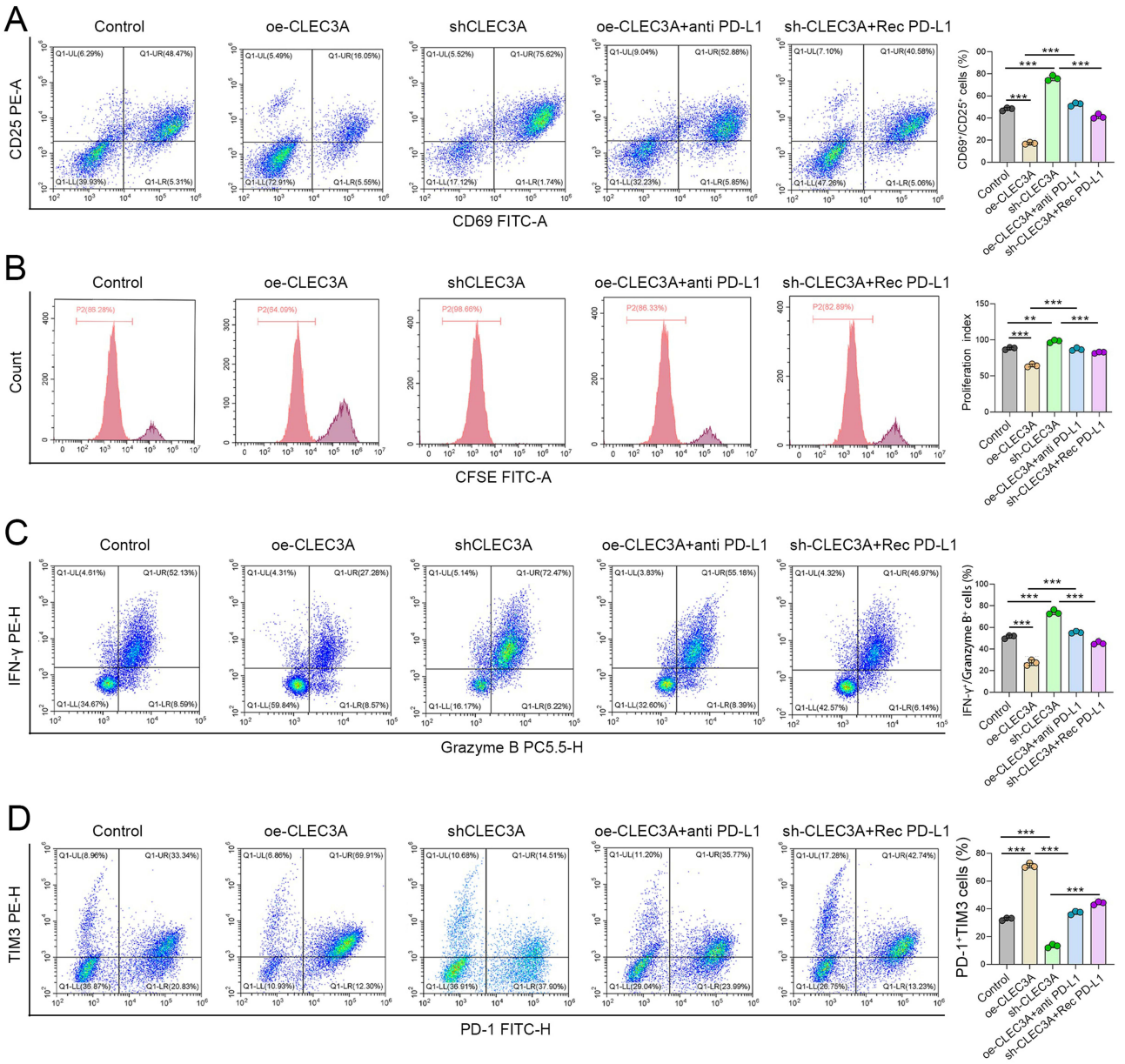

Figure 10 CLEC3A regulates CD8+ T cell function via PD-L1 in MCF-7 cells. (**A**) Flow cytometry analysis and quantification of CD8+ T cell activation (CD69+/CD25+) in different groups. (**B**) Analysis and quantification of CD8+ T cell proliferation (CFSE dilution). (**C**) Flow cytometry analysis and quantification of IFN-γ and Granzyme B production by CD8+ T cells. (**D**) Flow cytometry analysis and quantification of exhausted PD-1+TIM3+ T cell proportions. oe-CLEC3A-transfected MCF-7 cells were treated with 10 μg/mL anti-PD-L1 antibodies, and sh-CLEC3A-transfected MCF-7 cells were treated with 5 μg/mL recombinant PD-L1 protein. **p<0.01, ***p<0.001.

of cell proliferation markers such as CCND1, MYC, E2F1, and PCNA, and promotes the expression of CDKN1A, while CLEC3A overexpression produces the opposite effect. These results suggest that CLEC3A may regulate cell cycle checkpoints while promoting cell proliferation and potentially plays a carcinogenic role in luminal BC.

The prognosis of BC is not only related to biological characteristics but also to the TME. In luminal BC, a high proportion of infiltrating immune cells predicts a poorer prognosis, suggesting that effective immune escape may be an important factor influencing luminal BC recurrence.[23] CLEC3A is an immune-related gene in lung squamous cell carcinoma[20] and is also a core gene associated with immune cells in BC.[17] Our investigation into the immune-related effects of CLEC3A shows that it can influence key immune molecules in the BC tumor microenvironment. Specifically, CLEC3A knockout leads to an increase in the expression of immune-related factors, including CXCL10, CCL2, IL2,

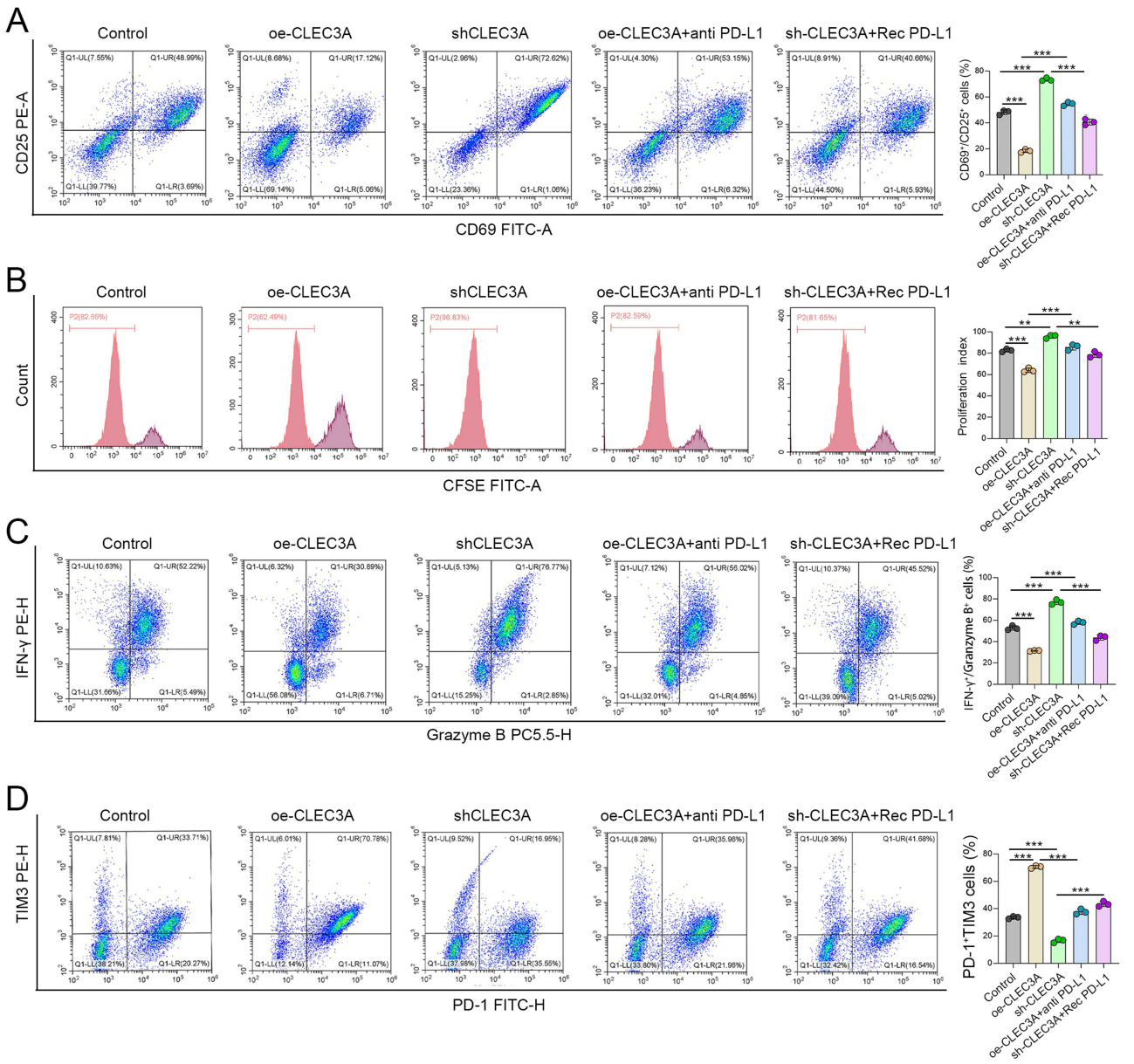

Figure 11 CLEC3A regulates CD8+ T cell function via PD-L1 in BT-474 cells. (**A**) Flow cytometry analysis and quantification of CD8+ T cell activation (CD69+/CD25+) in different groups. (**B**) Analysis and quantification of CD8+ T cell proliferation (CFSE dilution). (**C**) Flow cytometry analysis and quantification of IFN-γ and Granzyme B production by CD8+ T cells. (**D**) Flow cytometry analysis and quantification of exhausted PD-1+TIM3+ T cell proportions. oe-CLEC3A-transfected BT-474 cells were treated with 10 μg/mL anti-PD-L1 antibodies, and sh-CLEC3A-transfected BT-474 cells were treated with 5 μg/mL recombinant PD-L1 protein. **p<0.01, ***p<0.001.

IFNG, and STAT1, while CLEC3A overexpression inhibits the expression of these factors. These molecules are known to play crucial roles in promoting T-cell recruitment, activation, and anti-tumor immunity. CXCL10-positive BC shows higher $CD8^+$ immune cell infiltration.[24] In luminal BC, CCL2 is associated with the infiltration of tumor-associated macrophages, and increased CCL2 release enhances angiogenesis within macrophages.[25] IL-2 stimulates anti-cancer immunity and is one of the earliest cytokines used in cancer therapy.[26] IFNG is a crucial helper for CD8+ T cell cytotoxicity and can edit the BC microenvironment to promote stemness, disease progression, and resistance to immunotherapy.[27] STAT1 drives immune surveillance in BC.[28] We hypothesize that CLEC3A may participate in regulating the immune landscape of BC by inhibiting the activation of anti-tumor immunity.

The efficacy and safety of immunotherapy in luminal BC have been tested in several ongoing clinical trials.[10,29] As maintenance therapy, anti-PD-L1 antibodies have been shown to significantly improve OS in luminal BC compared to

chemotherapy.[30] This study found no significant correlation between CLEC3A and the PD-L1 encoding gene CD274, and changes in CLEC3A expression did not significantly affect PD-L1 mRNA levels. However, CLEC3A knockout significantly reduced PD-L1 protein expression, and proteasome inhibition restored PD-L1 levels. This suggests that CLEC3A may regulate the stability of PD-L1 protein in BC cells via the ubiquitination pathway, thereby affecting immune escape mechanisms. Previous studies have shown that ubiquitination enhances the immunosuppressive activity of PD-L1, thereby weakening the immune evasion ability of tumor cells.[31] In our co-culture experiments, CLEC3A knockout significantly enhanced the cytotoxic activity of $CD8^+$ T cells, as evidenced by increased proportions of $CD8^+$-$Perforin^+$ and $CD8^+$-TNF^+ T cells, along with elevated secretion of cytokines such as IL-2 and TNF-γ. In contrast, CLEC3A overexpression significantly suppressed $CD8^+$ T cell function, indicating that high levels of CLEC3A may inhibit anti-tumor immune responses. Importantly, our results demonstrated that CLEC3A-driven PD-L1 stabilization directly affected CD8+ T cell functional states. CLEC3A overexpression reduced CD8+ T cell activation, proliferation, and cytotoxic cytokine secretion, while these effects could be reversed by PD-L1 blockade. This finding aligns with a recent cross-sectional study, which reported that approximately 33% of BC patients exhibited high PD-L1 expression and low $CD8^+$ T cell counts.[32] Taken together, these results highlight a novel mechanism whereby CLEC3A promotes luminal BC progression by regulating PD-L1 to suppress CD8+ T cell–mediated anti-tumor immunity.

This study has certain limitations. First, the functional validation of CLEC3A was mainly performed in vitro using cell-based assays, without further verification in animal models. Although clinical luminal BC tissues supported the high expression of CLEC3A, the absence of in vivo experiments partially limits the translational relevance of our findings. Future studies incorporating animal models will be essential to confirm the role of CLEC3A in luminal BC progression and to provide more robust evidence for its potential as a prognostic biomarker and therapeutic target.

Conclusion

In conclusion, our study demonstrates that CLEC3A is associated with poor prognosis in luminal BC. CLEC3A promotes the malignant characteristics of BC cells by regulating cell proliferation and the immune microenvironment. Furthermore, CLEC3A affects PD-L1 stability through ubiquitination, contributing to immune escape. These findings suggest that CLEC3A may be a potential therapeutic target for improving anti-tumor immune responses in luminal BC.

Data Sharing Statement

The datasets generated during and/or analyzed during the current study are available from the corresponding author on reasonable request.

Ethics Approval

The Ethics Committee of The First Affiliated Hospital of Bengbu Medical University deemed that this research is based on open-source data, so the need for ethics approval was waived.

Funding

This work was supported by the following grants: Key Projects of Natural Science Research in Higher Education Institutions in Anhui Province (No. KJ2021A0815); Open Subjects of Scientific Research Platform of Anhui Biochemical Engineering Centre [No. 2023SYKFZ06]; Natural Science Key Projects of Bengbu Medical College (No. 2021byzd121).

Disclosure

The authors report no conflict of interest.

References

1. Sung H, Ferlay J, Siegel RL, et al. Global cancer statistics 2020: GLOBOCAN estimates of incidence and mortality worldwide for 36 cancers in 185 countries. *CA Cancer J Clin*. 2021;71(3):209–249. doi:10.3322/caac.21660

2. Cui Y, Li Y, Xu Y, et al. SLC7A11 protects luminal A breast cancer cells against ferroptosis induced by CDK4/6 inhibitors. *Redox Biol*. 2024;76:103304. doi:10.1016/j.redox.2024.103304
3. Niu Z, Wu J, Zhao Q, Zhang J, Zhang P, Yang Y. CAR-based immunotherapy for breast cancer: peculiarities, ongoing investigations, and future strategies. *Front Immunol*. 2024;15:1385571. doi:10.3389/fimmu.2024.1385571
4. Zhao M, Jiang Y, Kong X, et al. The analysis of plasma proteomics for luminal A breast cancer. *Cancer Med*. 2024;13(23):e70470. doi:10.1002/cam4.70470
5. Zhang H, Ma S, Wang Y, et al. Development of an obesity-related multi-gene prognostic model incorporating clinical characteristics in luminal breast cancer. *Iscience*. 2024;27(3):109133. doi:10.1016/j.isci.2024.109133
6. Lai H, Liu Y, Gong Y, Zong C, Zeng W, Chen H. Expression of SIGLEC15 correlates with tumor immune infiltration, molecular subtypes, and breast cancer progression. *PLoS One*. 2024;19(11):e0313561. doi:10.1371/journal.pone.0313561
7. Meng Y, Zhou D, Luo Y, Chen J, Li H. An estrogen-regulated long non-coding RNA NCALD promotes luminal breast cancer proliferation by activating GRHL2. *Cancer Cell Int*. 2024;24(1):49. doi:10.1186/s12935-024-03245-0
8. Seeing practice. Vet Rec. 1986;119(13)337–338. doi:10.1136/vr.119.13.337
9. He Y, Jiang Z, Chen C, Wang X. Classification of triple-negative breast cancers based on Immunogenomic profiling. *J Exp Clin Cancer Res*. 2018;37(1):327. doi:10.1186/s13046-018-1002-1
10. Dieci MV, Guarneri V, Tosi A, et al. Neoadjuvant chemotherapy and immunotherapy in luminal b-like breast cancer: results of the phase II GIADA trial. *Clin Cancer Res*. 2022;28(2):308–317. doi:10.1158/1078-0432.CCR-21-2260
11. Bernardis LL, McEwen G, Kodis M, Feldman MJ. Somatic, metabolic and endocrine correlates of set point recovery in food-restricted and ad lib-fed weanling rats with dorsomedial hypothalamic lesions. *Physiol Behav*. 1986;37(6):875–884. doi:10.1016/S0031-9384(86)80007-5
12. Hsu JM, Li CW, Lai YJ, Hung MC. Posttranslational modifications of PD-L1 and their applications in cancer therapy. *Cancer Res*. 2018;78(22):6349–6353. doi:10.1158/0008-5472.CAN-18-1892
13. Zhu D, Xu R, Huang X, et al. Deubiquitinating enzyme OTUB1 promotes cancer cell immunosuppression via preventing ER-associated degradation of immune checkpoint protein PD-L1. *Cell Death Differ*. 2021;28(6):1773–1789. doi:10.1038/s41418-020-00700-z
14. Chen X, Sun H, Yang C, et al. Bioinformatic analysis and experimental validation of six cuproptosis-associated genes as a prognostic signature of breast cancer. *PeerJ*. 2024;12:e17419. doi:10.7717/peerj.17419
15. Triulzi T, Giussani M, Maffioli E, et al. Proteomic landscape of decellularized breast carcinomas identifies C-type lectin domain family 3 member A as a driver of cancer aggressiveness. *NPJ Breast Cancer*. 2025;11(1):51. doi:10.1038/s41523-025-00769-0
16. Ni J, Peng Y, Yang FL, Xi X, Huang XW, He C. Overexpression of CLEC3A promotes tumor progression and poor prognosis in breast invasive ductal cancer. *Onco Targets Ther*. 2018;11:3303–3312. doi:10.2147/OTT.S161311
17. Chen X, Wang Y, Li Y, Liu G, Liao K, Song F. Identification of immune-related cells and genes in the breast invasive carcinoma microenvironment. *Aging*. 2022;14(3):1374–1388. doi:10.18632/aging.203879
18. Kaur D, Arora C, Raghava GPS. Prognostic biomarker-based identification of drugs for managing the treatment of endometrial cancer. *Mol Diagn Ther*. 2021;25(5):629–646. doi:10.1007/s40291-021-00539-1
19. Miki M, Oono T, Fujimori N, et al. CLEC3A, MMP7, and LCN2 as novel markers for predicting recurrence in resected G1 and G2 pancreatic neuroendocrine tumors. *Cancer Med*. 2019;8(8):3748–3760. doi:10.1002/cam4.2232
20. Pu J, Teng Z, Yang W, et al. Construction of a prognostic model for lung squamous cell carcinoma based on immune-related genes. *Carcinogenesis*. 2023;44(2):143–152. doi:10.1093/carcin/bgac098
21. Ren C, Pan R, Hou L, et al. Suppression of CLEC3A inhibits osteosarcoma cell proliferation and promotes their chemosensitivity through the AKT1/mTOR/HIF1alpha signaling pathway. *Mol Med Rep*. 2020;21(4):1739–1748. doi:10.3892/mmr.2020.10986
22. Ma Y, Huang X, Wang Y, et al. NNMT/1-MNA promote cell-cycle progression of breast cancer by targeting UBC12/Cullin-1-mediated degradation of P27 proteins. *Adv Sci*. 2024;11(9):e2305907. doi:10.1002/advs.202305907
23. Anabel Sinberger L, Zahavi T, Sonnenblick A, Salmon-Divon M. Coexistent ARID1A-PIK3CA mutations are associated with immune-related pathways in luminal breast cancer. *Sci Rep*. 2023;13(1):20911. doi:10.1038/s41598-023-48002-x
24. Kim M, Choi HY, Woo JW, Chung YR, Park SY. Role of CXCL10 in the progression of in situ to invasive carcinoma of the breast. *Sci Rep*. 2021;11(1):18007. doi:10.1038/s41598-021-97390-5
25. Svensson S, Abrahamsson A, Rodriguez GV, et al. CCL2 and CCL5 are novel therapeutic targets for estrogen-dependent breast cancer. *Clin Cancer Res*. 2015;21(16):3794–3805. doi:10.1158/1078-0432.CCR-15-0204
26. Chulpanova DS, Gilazieva ZE, Kletukhina SK, et al. Cytochalasin B-induced membrane vesicles from human mesenchymal stem cells over-expressing IL2 are able to stimulate CD8(+) T-killers to kill human triple negative breast cancer cells. *Biology*. 2021;10(2):141. doi:10.3390/biology10020141
27. Galassi C, Galluzzi L. Cancer stem cell immunoediting by IFNgamma. *Cell Death Dis*. 2023;14(8):538. doi:10.1038/s41419-023-06079-2
28. Ahn R, Sabourin V, Bolt AM, et al. The Shc1 adaptor simultaneously balances Stat1 and Stat3 activity to promote breast cancer immune suppression. *Nat Commun*. 2017;8:14638. doi:10.1038/ncomms14638
29. Adams S, Othus M, Patel SP, et al. A multicenter phase II trial of ipilimumab and nivolumab in unresectable or metastatic metaplastic breast cancer: cohort 36 of dual anti-CTLA-4 and anti-PD-1 blockade in rare tumors (DART, SWOG S1609). *Clin Cancer Res*. 2022;28(2):271–278. doi:10.1158/1078-0432.CCR-21-2182
30. Bachelot T, Filleron T, Bieche I, et al. Durvalumab compared to maintenance chemotherapy in metastatic breast cancer: the randomized phase II SAFIR02-BREAST IMMUNO trial. *Nat Med*. 2021;27(2):250–255. doi:10.1038/s41591-020-01189-2
31. Dong LF, Chen FF, Fan YF, Zhang K, Chen HH. circ-0000512 inhibits PD-L1 ubiquitination through sponging miR-622/CMTM6 axis to promote triple-negative breast cancer and immune escape. *J Immunother Cancer*. 2023;11(6):e005461. doi:10.1136/jitc-2022-005461
32. Kazmi S, Shawana S, Jamal N. PD-L1 and CD8+ T cell evaluation in breast cancers and their correlation with clinicopathological parameters. *J Pak Med Assoc*. 2024;74(7):1274–1279. doi:10.47391/JPMA.10567

Breast Cancer: Targets and Therapy

Dovepress
Taylor & Francis Group

Publish your work in this journal

Breast Cancer - Targets and Therapy is an international, peer-reviewed open access journal focusing on breast cancer research, identification of therapeutic targets and the optimal use of preventative and integrated treatment interventions to achieve improved outcomes, enhanced survival and quality of life for the cancer patient. The manuscript management system is completely online and includes a very quick and fair peer-review system, which is all easy to use. Visit http://www.dovepress.com/testimonials.php to read real quotes from published authors.

Submit your manuscript here: https://www.dovepress.com/breast-cancer—targets-and-therapy-journal